2023 62nd IEEE Conference on Decision and Control (CDC)
December 13-15, 2023. Marina Bay Sands, Singapore

Multiple Output Responses Decoupling: with Application to Vibration Suppression of Optical Tables

C.H. Lee, *Student Member, IEEE* and F.C. Wang*, *Senior Member, IEEE*

Abstract— **This paper proposes a novel control theorem called multiple output response decoupling (MORD) and applies it to optical-table vibration control. Optical tables need to isolate environmental vibrations by limited suspension travels. Soft suspensions can significantly isolate ground disturbances but need large strut displacements, while stiff suspensions can reduce suspension displacements but allow significant table vibrations. Passive suspensions are usually trade-offs between these conflicting requirements. Though active suspensions could relieve the compromises, the coupling system dynamics might cause difficulties in control designs. Therefore, this paper proposes the MORD theorem, which allows simultaneous performance improvement by independent control design. First, we review the disturbance response decoupling (DRD) theorem and simplify it as the output response decoupling (ORD) lemma. We then develop the MORD theorem, which can integrate independent ORD control designs without affecting each other. Finally, we apply the MORD theorem to the optical table systems. We design optimal controllers to suppress ground disturbances and other optimal controllers to minimize strut travels. We then integrate these controllers to achieve optimal performance simultaneously as the individual designs with the MORD control design.**

I. Introduction

Control design for multivariable systems is challenging because the controllers that improve particular performance specifications might degrade others. Therefore, multivariable control design is usually a compromise between various performance requirements. For example, vehicle suspensions must be soft to improve ride comfort or stiff to enhance handling maneuvers. Optical tables must suppress environmental vibrations for precision systems using limited suspension spaces. For instance, TMCTM applied passive springs and dampers to isolate ground disturbances [1], where the parameter settings are trade-offs between multiple system performances. For example, soft suspensions could repress ground disturbances but need significant strut travels, while stiff suspensions could reduce suspension strokes but introduce noteworthy table vibrations. Many studies [2-4] applied active optical tables to improve system performance. Nevertheless, the coupling system dynamics might increase the difficulties in active control designs.

Researchers have proposed decoupling techniques for multivariable control systems. For example, Hayakawa [5] applied decoupled control to improve automobile responses to road disturbances. Bronowicki [6] applied eigenvalue decomposition to decouple a multivariable control system into six single-input single-output systems. Wang [7] decoupled active front steering and suspensions using inverse dynamics and neural networks. Jamshidifar [8] decoupled the motion equations of a robot to minimize its disturbance responses.

Inspired by the coupling dynamics and multiple performance requirements for multivariable systems, Smith and Wang [9] proposed the disturbance response decoupling (DRD) theorem, which could keep specific transmission paths unchanged while improving others by feedback control. For example, they applied soft suspensions for vehicles to enhance ride comfort and optimized dynamic tire loads by active elements without changing the satisfied ride comfort [9, 10]. Wang et al. [11] implemented DRD control to optical tables, using soft parts to isolate ground disturbances while suppressing machine vibrations by voice coil motors (VCMs). Considering the transient responses, Wang et al. [12] proposed the inverse DRD control, restraining machine vibrations by stiff passive suspensions and suppressing ground disturbances by piezoelectric transducers (PZTs).

The DRD theorem provides a control structure to parameterize all stabilizing controllers, which can keep particular transmission paths unchanged while improving others. However, adjusting all system outputs independently and concurrently remains unsolved. This paper answers this problem by proposing the multiple output response decoupling (MORD) theorem, which allows us to conduct independent control designs for different system outputs and integrate them to improve all system performance as the individual designs.

This paper is organized as follows: Section 2 develops the MORD theorem. We review the DRD theorem and simplify it as the output responses decoupling (ORD) lemma, which allows us to shape particular system outputs without affecting others. We then propose the MORD theorem, which could integrate multiple ORD designs to improve system performance simultaneously as the individual ORD designs. Section 3 applies the MORD theorem to an optical table system. We design ORD controllers to improve individual output responses and integrate these controllers to improve all concerned outputs independently and simultaneously. Finally, we conclude in Section 4.

II. Multiple Output Response Decoupling

This section develops the MORD theorem. We first review the DRD theorem. Consider the linear fractional transformation (LFT) model, as shown in Figure 1, where

$$\begin{bmatrix} z \\ y \end{bmatrix} = P\begin{bmatrix} w \\ u \end{bmatrix} = \begin{bmatrix} P_{11} & P_{12} \\ P_{21} & P_{22} \end{bmatrix}\begin{bmatrix} w \\ u \end{bmatrix}, \quad (1)$$

C.H. Lee and F.C. Wang* are with the Department of Mechanical Engineering, National Taiwan University, (*corresponding author to provide phone: +886-2-33662680; E-mail: fcw@ntu.edu.tw).

979-8-3503-0123-6/23/$31.00 ©2023 IEEE

in which w is the system input, z is the system output, y is the feedback measurement, and u is the control. Suppose $w=\begin{bmatrix} w_1 & w_2 \end{bmatrix}^T$ and $z=\begin{bmatrix} z_1 & z_2 \end{bmatrix}^T$. The generalized plant P can be conformally partitioned such that

$$\begin{bmatrix} \begin{bmatrix} \hat{z}_1 \\ \hat{z}_2 \end{bmatrix} \\ \hat{y} \end{bmatrix} = \begin{bmatrix} \begin{bmatrix} \hat{P}_{11,11} & \hat{P}_{11,12} \\ \hat{P}_{11,21} & \hat{P}_{11,22} \end{bmatrix} & \begin{bmatrix} \hat{P}_{12,1} \\ \hat{P}_{12,2} \end{bmatrix} \\ \begin{bmatrix} \hat{P}_{21,1} & \hat{P}_{21,2} \end{bmatrix} & \hat{P}_{22} \end{bmatrix} \begin{bmatrix} \begin{bmatrix} \hat{w}_1 \\ \hat{w}_2 \end{bmatrix} \\ \hat{u} \end{bmatrix} \tag{2}$$

where $w_1 \in \mathbb{R}^{m_1}$, $w_2 \in \mathbb{R}^{m_2}$, $u \in \mathbb{R}^{m_3}$, $z_1 \in \mathbb{R}^{p_1}$, $z_2 \in \mathbb{R}^{p_2}$ and $y \in \mathbb{R}^{p_3}$. The superscript ˆ denotes the Laplace transform of the signal.

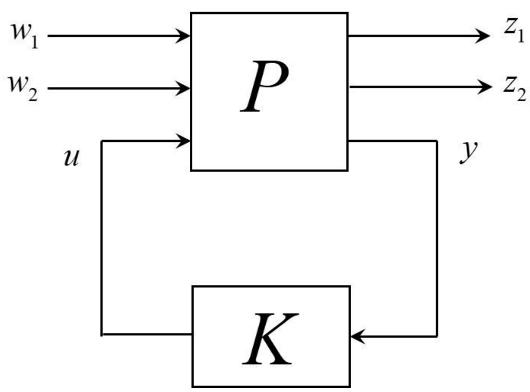

Figure 1. The generalized LFT form

Suppose P_{22} can be coprime factorised as $P_{22}=NM^{-1}=\tilde{M}^{-1}\tilde{N}$, where $M,N,\tilde{M},\tilde{N} \in \mathbb{RH}_\infty$, all stabilizing controllers can be parameterized as [13]:

$$\begin{aligned} K &= \left(Y-MQ\right)\left(X-NQ\right)^{-1} \\ &= \left(\tilde{X}-Q\tilde{N}\right)^{-1}\left(\tilde{Y}-Q\tilde{M}\right) \end{aligned} \tag{3}$$

for $Q \in \mathbb{RH}_\infty^{m_3 \times p_3}$. $X,Y,\tilde{X},\tilde{Y} \in \mathbb{RH}_\infty$ and satisfy the following Bezout identity:

$$\begin{bmatrix} \tilde{X} & -\tilde{Y} \\ -\tilde{N} & \tilde{M} \end{bmatrix} \begin{bmatrix} M & Y \\ N & X \end{bmatrix} = I$$

Without loss of generality, we can set a stabilizing controller $K_0 = YX^{-1} = \tilde{X}^{-1}\tilde{Y}$ with $Q=0$. Furthermore, when P is stable, we can set $\tilde{N}=N=P_{22}$ and let $\tilde{Y}=0$ and $Y=0$ in the Bezout identity and let $K_0=0$. Suppose $r_2 \le \min(p_1+p_2,\, m_3)$ and $r_3 \le \min(m_1+m_2,\, p_3)$, the DRD theorem when P is stable is described as follows:

Theorem 1 (Disturbance responses decoupling) [9, 10]:

When P is stable, all stabilizing controllers which let $T_{\hat{w}_1 \to \hat{z}_1} = \hat{P}_{11,11}$ are given by Eq.(3) with

$$Q = \begin{bmatrix} V_1 \\ V_2 \end{bmatrix}^{-1} \begin{bmatrix} Q_1 \tilde{U}_2 \\ Q_2 \end{bmatrix} = \begin{bmatrix} \tilde{V}_1 & \tilde{V}_2 \end{bmatrix} \begin{bmatrix} Q_1 \tilde{U}_2 \\ Q_2 \end{bmatrix} \tag{4}$$

for $Q_1 \in \mathbb{RH}_\infty^{r_2 \times (p_3 - r_3)}$, $Q_2 \in \mathbb{RH}_\infty^{(m_3 - r_2) \times p_3}$, $\tilde{U}_2 \in \mathbb{RH}_\infty^{(p_3 - r_3) \times p_3}$, $V_1 \in \mathbb{RH}_\infty^{r_2 \times m_3}$ and $V_2 \in \mathbb{RH}_\infty^{(m_3 - r_2) \times m_3}$, where $\begin{bmatrix} V_1^T & V_2^T \end{bmatrix}$ is unimodular.

(proof) See [9].

We can simplify the DRD theorem as the following ORD lemma, which could modify specific output responses without changing others.

Lemma 1 (Output response decoupling):

Suppose P is stable, the stabilizing controller in (3) with $Q = \tilde{V}_2^{z_1} Q_2^{z_1}$ can modify $T_{\hat{w} \to \hat{z}_1}$ and keep $T_{\hat{w} \to \hat{z}_2} = \begin{bmatrix} \hat{P}_{11,21} & \hat{P}_{11,22} \end{bmatrix}$, as shown in Figure 2, where $Q_2^{z_1} \in RH_\infty^{(m_3 - \bar{r}_2) \times p_3}$, $\tilde{V}_2^{z_1} \in RH_\infty^{m_3 \times (m_3 - \bar{r}_2)}$ is a right annihilator of $\hat{P}_{12,2}$, and $\bar{r}_2 \le \min(p_2,\, m_3)$.

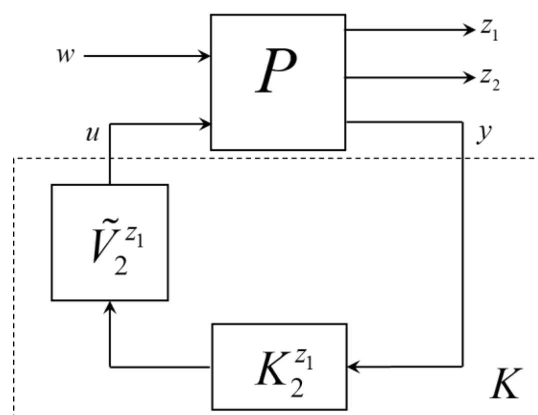

Figure 2. The ORD control structure.

We now introduce the MORD theorem, where multiple ORD controllers can be integrated to modify all system outputs simultaneously as the individual ORD designs.

Theorem 2 (Multiple output response decoupling):

Let P be stable with $z = \begin{bmatrix} z_1 & z_2 & \cdots & z_p \end{bmatrix}^T$ and $r_3 = p_3$. Then $T_{\hat{w} \to \hat{z}_j}$ can be shaped independently and simultaneously by the control structure of Figure 3, where $K_2^{z_j}$ and $\tilde{V}_2^{z_j}$ represent the ORD design for z_j.

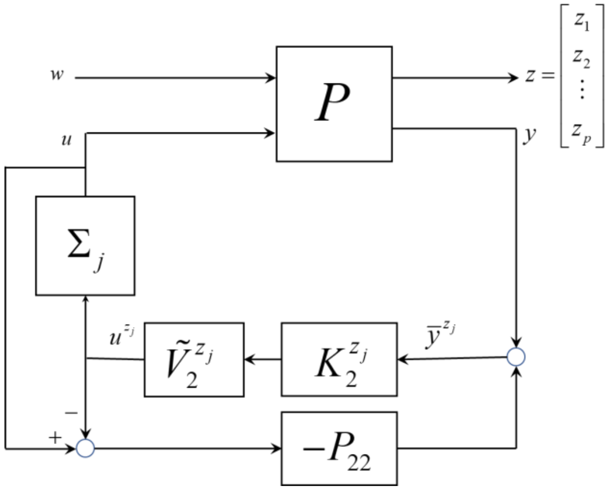

Figure 3. The MORD control structure.

Example:

Considered the following system:

$$\hat{P}_{11}=\begin{bmatrix}\frac{1}{s+1}\\ \frac{1}{s+2}\\ \frac{1}{s+3}\end{bmatrix},\ \hat{P}_{12}=\begin{bmatrix}\frac{1}{s+5} & \frac{1}{s+9} & \frac{1}{s+13}\\ \frac{1}{s+6} & \frac{1}{s+10} & \frac{1}{s+14}\\ \frac{1}{s+7} & \frac{1}{s+11} & \frac{1}{s+15}\end{bmatrix},$$

$$\hat{P}_{21}=\begin{bmatrix}\frac{1}{s+4}\end{bmatrix},\ \hat{P}_{22}=\begin{bmatrix}\frac{1}{s+8} & \frac{1}{s+12} & \frac{1}{s+16}\end{bmatrix}.$$

First, we derived the ORD filters as follows:

$$\tilde{V}_2^{z_1}=\frac{1}{H_1(s)}\begin{bmatrix}(s+6)(s+7)\\ -2(s+10)(s+11)\\ (s+14)(s+15)\end{bmatrix},$$

$$\tilde{V}_2^{z_2}=\frac{1}{H_2(s)}\begin{bmatrix}(s+5)(s+7)\\ -2(s+9)(s+11)\\ (s+13)(s+15)\end{bmatrix},$$

$$\tilde{V}_2^{z_3}=\frac{1}{H_3(s)}\begin{bmatrix}(s+5)(s+6)\\ -2(s+9)(s+10)\\ (s+13)(s+14)\end{bmatrix}.$$

where $H_1(s)$, $H_2(s)$ and $H_3(s)$ are Hurwitz polynomials such that $\tilde{V}_2^{z_1}$, $\tilde{V}_2^{z_2}$, $\tilde{V}_2^{z_3}\in RH_\infty$. Second, we applied the MATLAB command *h2syn* to derive the optimal controllers $K_2^{z_j}$ by the weighted plants $P\begin{bmatrix}I & \tilde{V}_2^{z_j}\end{bmatrix}^T$ $i=1,\ 2,\ 3$. Third, we implemented the ORD structure with the weighted controllers $K=\tilde{V}_2^{z_j}K_2^{z_j}$ to the original plant P. The results are shown in Figure 4.

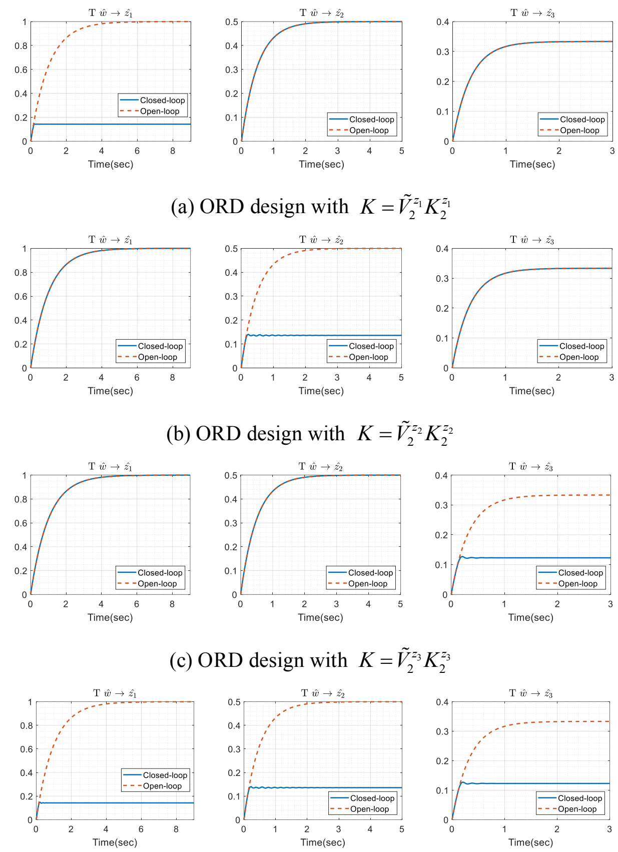

(a) ORD design with $K=\tilde{V}_2^{z_1}K_2^{z_1}$

(b) ORD design with $K=\tilde{V}_2^{z_2}K_2^{z_2}$

(c) ORD design with $K=\tilde{V}_2^{z_3}K_2^{z_3}$

(d) MORD design

Figure 4. The ORD and MORD control design for the example.

As shown in Figure 4, the ORD control with $K=\tilde{V}_2^{z_i}K_2^{z_i}$ changed $T_{\hat{w}\to\hat{z}_i}$ but left $T_{\hat{w}\to\hat{z}_j}$ the same as the open-loop for $i=1,\ 2,\ 3$ and $j\neq i$. Finally, we implemented the MORD control. The results are shown in Figure 4(d), where $T_{\hat{w}\to\hat{z}_1}$, $T_{\hat{w}\to\hat{z}_2}$, and $T_{\hat{w}\to\hat{z}_3}$ were the same as the individual ORD designs. The multiple output responses could be independently designed and integrated without cross-influence.

III. MORD Control Design for an Optical Table

We apply the MORD theorem to an optical-table model, as shown in Figure 5. The system dynamics can be described as follows:

$$\begin{aligned}
&m_s\ddot{z}_s=-f^1-f^2-f^3-f^4,\\
&I_\phi\ddot{z}_\phi=-l_1f^1+l_1f^2-l_2f^3+l_2f^4,\\
&I_\theta\ddot{z}_\theta=-t_1f^1-t_1f^2+t_2f^3+t_2f^4, \qquad (5)\\
&m_u^1\ddot{z}_u^1=F_A^1+f^1-f_r^1,\ \ m_u^2\ddot{z}_u^2=F_A^2+f^2-f_r^2,\\
&m_u^3\ddot{z}_u^3=F_A^3+f^3-f_r^3,\ \ m_u^3\ddot{z}_u^4=F_A^4+f^4-f_r^4,
\end{aligned}$$

where the tire forces are $f_r^i=\Theta_1^i(z_u^i-z_r^i)$ and the suspension forces are $f^i=\Theta_3^i(z_a^i-z_u^i)+\Theta_2^i(z_s^i-z_u^i)$ and for $i=1,2,3,4$.

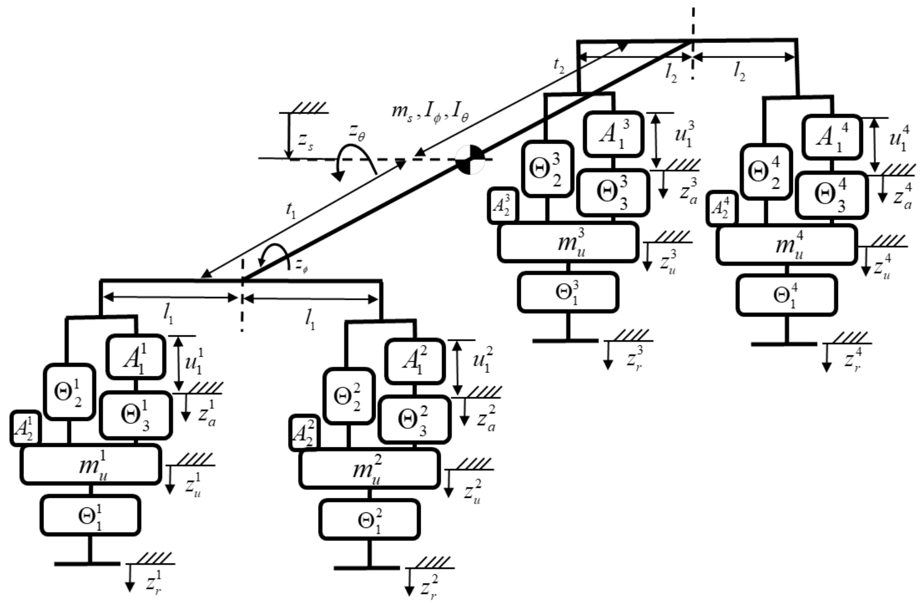

Figure 5. The full-optical-table model.

z_s^i represents the table displacements at the i-th corners:

$$z_s^1 = z_s + l_1 z_\phi + t_1 z_\theta,\ z_s^2 = z_s - l_1 z_\phi + t_1 z_\theta,$$
$$z_s^3 = z_s + l_2 z_\phi - t_2 z_\theta,\ z_s^4 = z_s - l_2 z_\phi - t_2 z_\theta. \tag{6}$$

Suppose the concerned system outputs are the table movements ($z_s, z_\phi, \text{and}\, z_\theta$) and the strut travels ($D^i = z_s^i - z_u^i$, for i=1, 2, 3, 4). Four PZTs control the suspension displacements at the four corners as $z_a^i - z_s^i = \gamma u_1^i$, for i=1, 2, 3, 4 according to the PZT control commands u_1^i, where γ represents the PZT dynamics. Four VCMs apply forces $F_A^i = \kappa u_2^i$ on m_u^i according to the VCM control commands u_2^i, where κ is the VCM dynamics.

Taking the Laplace transform of equations (5-6). The system LFT form is as Eq.(1) with $w=\left[z_r^1, z_r^2, z_r^3, z_r^4\right]^T$, $z=\left[z_s, z_\phi, z_\theta, D^1, D^2, D^3, D^4\right]^T$, $y=\left[z_s, z_\phi, z_\theta\right]^T$, and $u=\left[u_1^1, u_2^1, u_1^2, u_2^2, u_1^3, u_2^3, u_1^4, u_2^4\right]^T$.

We could further transfer the road disturbances (z_r^i) and suspension strokes (D^i) to the bounce, roll, and pitch components as follows:

$$\begin{bmatrix} z_r^b \\ z_r^\phi \\ z_r^\theta \end{bmatrix} = T_2 \begin{bmatrix} z_r^1 \\ z_r^2 \\ z_r^3 \\ z_r^4 \end{bmatrix} \text{ and } \begin{bmatrix} D^b \\ D^\phi \\ D^\theta \end{bmatrix} = T_2 \begin{bmatrix} D^1 \\ D^2 \\ D^3 \\ D^4 \end{bmatrix},$$

where

$$T_2 = \begin{bmatrix} \frac{t_2}{2(t_1+t_2)} & \frac{t_2}{2(t_1+t_2)} & \frac{t_1}{2(t_1+t_2)} & \frac{t_1}{2(t_1+t_2)} \\ \frac{l_1}{2(l_1^2+l_2^2)} & -\frac{l_1}{2(l_1^2+l_2^2)} & \frac{l_2}{2(l_1^2+l_2^2)} & -\frac{l_2}{2(l_1^2+l_2^2)} \\ \frac{1}{2(t_1+t_2)} & \frac{1}{2(t_1+t_2)} & -\frac{1}{2(t_1+t_2)} & -\frac{1}{2(t_1+t_2)} \end{bmatrix}.$$

The LFT form of the model can be modified in Figure 6.

Suppose the four legs are identical, i.e., $\Theta_1^i = \Theta_1$, $\Theta_2^i = \Theta_2$, $\Theta_3^i = \Theta_3$, and $m_u^i = m_u$ for i =1, 2, 3, 4. We can derive the ORD filters $\tilde{V}_2^{z_j'}$ for $z_j' \in \left\{\hat{z}_s, \hat{z}_\phi, \hat{z}_\theta, \hat{D}^b, \hat{D}^\phi, \hat{D}^\theta\right\}$, which could modify $T_{\hat{w}' \to \hat{z}_j'}$, without changing other system output responses.

Set the system parameters as follows [11]: $m_s = 280.32$kg, $m_u = 15.15$ kg, $I_\phi = 9.92$kgm^2, $I_\theta = 17.27$kgm^2, $\hat{\Theta}_1 = 2250s + 1.65\times10^4$, $\hat{\Theta}_2 = 96s + 2.12\times10^4$, $\hat{\Theta}_3 = 5.73\times10^4$, $l_1 = l_2 = 0.45$m, $t_1 = t_2 = 0.6$m, $\hat{\gamma} = 4.14\times10^{-6}$, and $\hat{\kappa} = 1.6$, we designed six ORD controllers $K_2^{z_j'}$ for the weighted plant $P'\left[I \ \ \tilde{V}_2^{z_j'}\right]^T$ and implemented the weighted ORD controllers $\tilde{V}_2^{z_j'} K_2^{z_j'}$ to the original plant P.

(1) The first ORD controller $K_2^{\hat{z}_s}$ minimized $\left\|T_{\hat{z}_r^b \to \hat{z}_s}\right\|_\infty$.

(2) The second ORD controller $K_2^{\hat{z}_\phi}$ minimized $\left\|T_{\hat{z}_r^\phi \to \hat{z}_\phi}\right\|_\infty$.

(3) The third ORD controller $K_2^{\hat{z}_\theta}$ minimized $\left\|T_{\hat{z}_r^\theta \to \hat{z}_\theta}\right\|_\infty$.

(4) The fourth ORD controller $K_2^{\hat{D}^b}$ minimized $\left\|T_{\hat{z}_r^b \to \hat{D}^b}\right\|_2$.

(5) The fifth ORD controller $K_2^{\hat{D}^\phi}$ minimized $\left\|T_{\hat{z}_r^\phi \to \hat{D}^\phi}\right\|_2$.

(6) The sixth ORD controller $K_2^{\hat{D}^\theta}$ minimized $\left\|T_{\hat{z}_r^\theta \to \hat{D}^\theta}\right\|_2$.

Finally, we implemented the MORD control structure with these ORD controllers. The results are shown in Table 1, where $T_{\hat{z}_r^b \to \hat{z}^b}, T_{\hat{z}_r^\phi \to \hat{z}_\phi}, T_{\hat{z}_r^\theta \to \hat{z}_\theta}, T_{\hat{z}_r^b \to \hat{D}^b}$, $T_{\hat{z}_r^\phi \to \hat{D}^\phi}$, and $T_{\hat{z}_r^\theta \to \hat{D}^\theta}$ are the same as the individual ORD designs. We could design separate controllers to enhance the system responses of particular outputs and integrate them to improve all output responses simultaneously.

IV. CONCLUSION

This paper has introduced the MORD theorem and applied it to optical table systems. We first simplified the DRD theorem as the ORD lemma and developed the MORD theorem. Then, we implemented the MORD structure into a full-table system. We conducted six ORD controls and integrated them to improve all concerned outputs as the individual ORD designs.

In the future, we will investigate on the combination of MIDD[14] and MORD theorems, where the controllers for each transmission path could be independently designed and integrated without cross-influences. Furthermore, we are approaching to build up an experimental model of the quarter-table system for demonstrating the feasibility and effectiveness of MORD control.

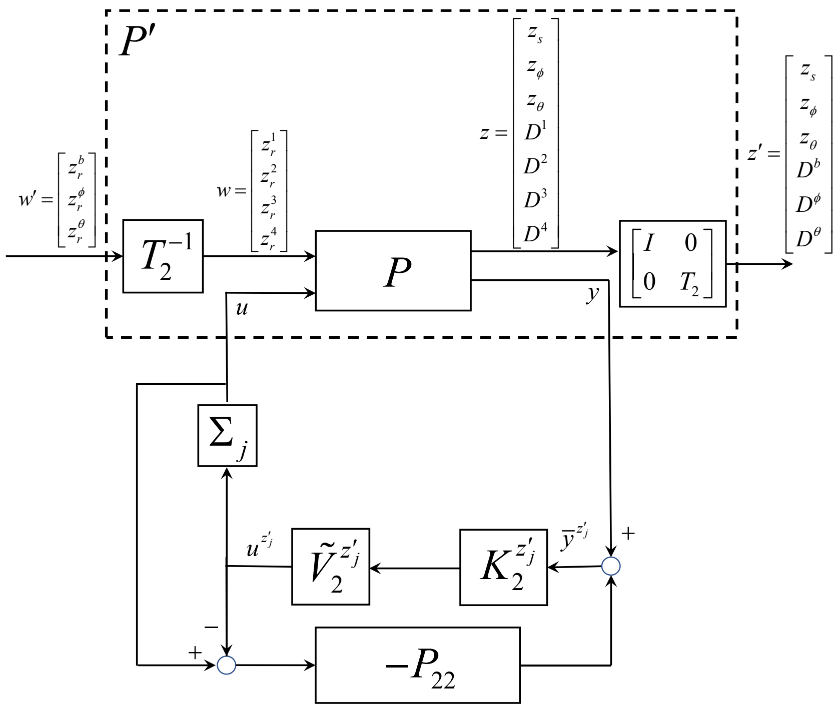

Figure 6. The MORD control for the full-table model.

Table 1. Performance of the full-table employing the ORD and MORD designs.

	Passive	$K_2^{\hat{z}_s}$ (imp%)	$K_2^{\hat{z}_\phi}$ (imp%)	$K_2^{\hat{z}_\theta}$ (imp%)	$K_2^{\hat{D}^b}$ (imp%)	$K_2^{\hat{D}^\phi}$ (imp%)	$K_2^{\hat{D}^\theta}$ (imp%)	MORD (imp%)
$\left\|T_{\hat{z}_r^b \to \hat{z}_s}\right\|_\infty$	1.3634 –	1.64×10^{-4} (99.99%)	1.3634 –	1.3634 –	1.3634 –	1.3634 –	1.3634 –	1.64×10^{-4} (99.99%)
$\left\|T_{\hat{z}_r^\phi \to \hat{z}_\phi}\right\|_\infty$	1.5777 –	1.5777 –	0.2148 (86.38%)	1.5777 –	1.5777 –	1.5777 –	1.5777 –	0.2148 (86.38%)
$\left\|T_{\hat{z}_r^\theta \to \hat{z}_\theta}\right\|_\infty$	1.8778 –	1.8778 –	1.8778 –	0.0779 (95.85%)	1.8778 –	1.8778 –	1.8778 –	0.0779 (95.85%)
$\left\|T_{\hat{z}_r^b \to \hat{D}^b}\right\|_2$	2.7258 –	2.7258 –	2.7258 –	2.7258 –	1.4736 (45.94%)	2.7258 –	2.7258 –	1.4736 (45.94%)
$\left\|T_{\hat{z}_r^\phi \to \hat{D}^\phi}\right\|_2$	2.8648 –	2.8648 –	2.8648 –	2.8648 –	2.8648 –	0.7476 (73.90%)	2.8648 –	0.7476 (73.90%)
$\left\|T_{\hat{z}_r^\theta \to \hat{D}^\theta}\right\|_2$	3.4213 –	3.4213 –	3.4213 –	3.4213 –	3.4213 –	3.4213 –	1.0914 (68.10%)	1.0914 (68.10%)

ACKNOWLEDGMENT

This research was financially supported by the Ministry of Science and Technology of Taiwan under Grand MOST 110-2221-E-002-167-.

REFERENCES

[1] TMC. "Products Series." https://www.techmfg.com/products (accessed 28 Feb. 2023, 2023).

[2] T. Kato, K. Kawashima, T. Funaki, K. Tadano, and T. Kagawa, "A new, high precision, quick response pressure regulator for active control of pneumatic vibration isolation tables," *Precision Engineering,* vol. 34, no. 1, pp. 43-48, 2010.

[3] P.-h. Chang, D. K. Han, Y.-h. Shin, and K.-j. Kim, "Effective suppression of pneumatic vibration isolators by using input–output linearization and time delay control," *Journal of Sound and Vibration,* vol. 329, no. 10, pp. 1636-1652, 2010.

[4] J.-S. Oh, Y.-M. Han, S.-B. Choi, V.-Q. Nguyen, and S.-J. Moon, "Design of a one-chip board microcontrol unit for active vibration control of a naval ship mounting system," *Smart materials and structures,* vol. 21, no. 8, p. 087001, 2012.

[5] K. Hayakawa, K. Matsumoto, M. Yamashita, Y. Suzuki, K. Fujimori, and H. Kimura, "Robust H∞-output feedback control of decoupled automobile active suspension systems," *IEEE Trans. Autom. Control.,* vol. 44, pp. 392-396, 1999.

[6] A. J. Bronowicki, "A layered vibration control strategy for space telescopes," in *Smart Structures and Materials 2003: Smart Structures and Integrated Systems*, 2003, vol. 5056: SPIE, pp. 487-496.

[7] C. Wang, W. Zhao, Z. Luan, Q. Gao, and K. Deng, "Decoupling control of vehicle chassis system based on neural network inverse system," *Mechanical Systems and Signal Processing,* vol. 106, pp. 176-197, 06/01 2018, doi: https://doi.org/10.1016/j.ymssp.2017.12.032.

[8] H. Jamshidifar, S. Khosravani, B. Fidan, and A. Khajepour, "Vibration Decoupled Modeling and Robust Control of Redundant Cable-Driven Parallel Robots," *IEEE/ASME Transactions on Mechatronics,* vol. 23, no. 2, pp. 690-701, 2018, doi: 10.1109/TMECH.2018.2793578.

[9] M. C. Smith and F.-C. Wang, "Controller parameterization for disturbance response decoupling: application to vehicle active suspension control," *IEEE Transactions on Control Systems Technology,* vol. 10, no. 3, pp. 393-407, 2002, doi: 10.1109/87.998029.

[10] F.-C. Wang and M. C. Smith, "Disturbance response decoupling and achievable performance with application to vehicle active suspension," *International Journal of Control,* vol. 75, no. 12, pp. 946-953, 2002.

[11] F.-C. Wang, C.-H. Yu, J. Tsai, and S.-H. Yang, "Decoupled robust vibration control of an optical table," *Journal of Vibration and Control,* vol. 20, pp. 38-50, 01/07 2012, doi: 10.1177/1077546312461369.

[12] F.-C. Wang and S.-Y. Wu, "Vibration suppression of an optical table with inverse disturbance response decoupling," *Journal of Vibration and Control,* vol. 22, no. 1, pp. 51-59, 2016, doi: 10.1177/1077546314528019.

[13] K. Zhou, J. C. Doyle, and K. Glover, *Robust and optimal control*. Prentice hall, 1996.

[14] F.-C. Wang and C.-H. Lee, "Multiple Input Disturbance Decoupling: with Application to Vehicle Suspension Design," in *SICE Annual Conference 2023*, Tsu, JAPAN, 2023.